

# Tunable, high-energy, mid-infrared, picosecond optical parametric generator based on CdSiP<sub>2</sub>

S. Chaitanya Kumar,<sup>1,\*</sup> M. Jelínek,<sup>2</sup> M. Baudisch,<sup>1</sup> K. T. Zawilski,<sup>3</sup> P. G. Schunemann,<sup>3</sup>  
V. Kubeček,<sup>2</sup> J. Biegert,<sup>1,4</sup> and M. Ebrahim-Zadeh<sup>1,4</sup>

<sup>1</sup>ICFO-Institut de Ciències Fotoniques, Mediterranean Technology Park, 08860 Castelldefels, Barcelona, Spain

<sup>2</sup>Czech Technical University, Faculty of Nuclear Sciences and Physical Engineering, Prague, Czech Republic

<sup>3</sup>BAE Systems, Inc., MER15-1813, P.O. Box 868, Nashua, New Hampshire 03061-0868, USA

<sup>4</sup>Institució Catalana de Recerca i Estudis Avançats (ICREA), Passeig Lluís Companys 23, Barcelona 08010, Spain  
[chaitanya.suddapalli@icfo.es](mailto:chaitanya.suddapalli@icfo.es)

**Abstract:** We report a tunable, high-energy, single-pass optical parametric generator (OPG) based on the nonlinear material, cadmium silicon phosphide, CdSiP<sub>2</sub>. The OPG is pumped by a cavity-dumped, passively mode-locked, diode-pumped Nd:YAG oscillator, providing 25 μJ pulses in 20 ps at 5 Hz. The pump energy is further boosted by a flashlamp-pumped Nd:YAG amplifier to 2.5 mJ. The OPG is temperature tunable over 1263–1286 nm (23 nm) in the signal and 6153–6731 nm (578 nm) in the idler. Using the single-pass OPG configuration, we have generated signal pulse energy as high as 636 μJ at 1283 nm, together with idler pulse energy of 33 μJ at 6234 nm, for 2.1 mJ of input pump pulse energy. The generated signal pulses have durations of 24 ps with a FWHM spectral bandwidth of 10.4 nm at central wavelength of 1276 nm. The corresponding idler spectrum has a FWHM bandwidth of 140 nm centered at 6404 nm.

©2012 Optical Society of America

**OCIS codes:** (190.4970) Parametric oscillators and amplifiers; (190.4400) Nonlinear optics, materials; (190.7110) Ultrafast nonlinear optics.

---

## References and links

1. G. Edwards, R. Logan, M. Copeland, L. Reinisch, J. Davidson, B. Johnson, R. Maciunas, M. Mendenhall, R. Ossoff, J. Tribble, J. Werkhaven, and D. O'day, "Tissue ablation by a free-electron laser tuned to the amide II band," *Nature* **371**(6496), 416–419 (1994).
2. J. Hildenbrand, J. Herbst, J. Wöllenstein, and A. Lambrecht, "Explosive detection using infrared laser spectroscopy," *Proc. SPIE* **7222**, 72220B (2009).
3. J. Zhang, J. Y. Huang, and Y. R. Shen, *Optical Parametric Generation and Amplification* (Harwood Academic Publishers, 1995).
4. M. Ebrahim-Zadeh and I. T. Sorokina, *Mid-Infrared Coherent Sources and Applications* (Springer, 2007).
5. J. Biegert, P. K. Bates, and O. Chalus, "New mid-IR light sources," *IEEE J. Sel. Top. Quant. Electron.-Ultrafast Sci. Technol* **18**(1), 531–540 (2012).
6. S. Chaitanya Kumar, A. Esteban-Martin, and M. Ebrahim-Zadeh, "Interferometric output coupling of ring optical oscillators," *Opt. Lett.* **36**(7), 1068–1070 (2011).
7. S. C. Kumar and M. Ebrahim-Zadeh, "High-power, fiber-laser-pumped, picosecond optical parametric oscillator based on MgO:sPPLT," *Opt. Express* **19**(27), 26660–26665 (2011).
8. D. N. Nikogosyan, *Nonlinear Optical Crystals: A Complete Survey* (Springer 2005).
9. K. T. Zawilski, P. G. Schunemann, T. C. Pollak, D. E. Zelmon, N. C. Fernelius, and F. K. Hopkins, "Growth and characterization of large CdSiP<sub>2</sub> single crystals," *J. Cryst. Growth* **312**(8), 1127–1132 (2010).
10. V. Petrov, F. Noack, I. Tunchev, P. Schunemann, and K. Zawilski, "The nonlinear coefficient d<sub>36</sub> of CdSiP<sub>2</sub>," *Proc. SPIE* **7197**, 71970M, 71970M-8 (2009).
11. V. Petrov, P. G. Schunemann, K. T. Zawilski, and T. M. Pollak, "Noncritical singly resonant optical parametric oscillator operation near 6.2 microm based on a CdSiP<sub>2</sub> crystal pumped at 1064 nm," *Opt. Lett.* **34**(16), 2399–2401 (2009).
12. V. Petrov, G. Marchev, P. G. Schunemann, A. Tyazhev, K. T. Zawilski, and T. M. Pollak, "Subnanosecond, 1 kHz, temperature-tuned, noncritical mid-infrared optical parametric oscillator based on CdSiP<sub>2</sub> crystal pumped at 1064 nm," *Opt. Lett.* **35**(8), 1230–1232 (2010).
13. A. Peremans, D. Lis, F. Cecchet, P. G. Schunemann, K. T. Zawilski, and V. Petrov, "Noncritical singly resonant synchronously pumped OPO for generation of picosecond pulses in the mid-infrared near 6.4 microm," *Opt. Lett.* **34**(20), 3053–3055 (2009).

14. S. Chaitanya Kumar, A. Agnesi, P. Dallochio, F. Pirzio, G. Reali, K. T. Zawilski, P. G. Schunemann, and M. Ebrahim-Zadeh, "Compact, 1.5 mJ, 450 MHz, CdSiP<sub>2</sub> picosecond optical parametric oscillator near 6.3 μm," *Opt. Lett.* **36**(16), 3236–3238 (2011).
15. O. Chalus, P. G. Schunemann, K. T. Zawilski, J. Biegert, and M. Ebrahim-Zadeh, "Optical parametric generation in CdSiP<sub>2</sub>," *Opt. Lett.* **35**(24), 4142–4144 (2010).
16. M. Jelínek and V. Kubeček, "15 ps quasi-continuously pumped passively mode-locked highly doped Nd:YAG laser in bounce geometry," *Laser Phys. Lett.* **8**, 657–660 (2011).
17. K. Kato, N. Umemura, and V. Petrov, "Sellmeier and thermo-optic dispersion formulas for CdSiP<sub>2</sub>," *J. Appl. Phys.* **109**(11), 116104 (2011).
18. A. Agnesi, E. Piccinini, G. C. Reali, and C. Solcia, "All-solid-state picosecond tunable source of near-infrared radiation," *Opt. Lett.* **22**(18), 1415–1417 (1997).
19. R. L. Byer, "Optical parametric oscillators," in *Quantum Electronics: A Treatise*, H. Rabin and C. L. Tang, eds. (Academic, 1975), pp. 587–702.

## 1. Introduction

The wavelength range between 5900 nm and 6600 nm in the mid-infrared (mid-IR) is of great interest for a variety of applications, including human surgery [1] and explosive detection [2]. In the absence of conventional solid-state lasers in this spectral range, tunable optical parametric generators (OPGs) [3], optical parametric oscillators (OPOs) [4], and optical parametric chirped pulse amplifiers (OPCPAs) [5] represent attractive alternatives for wavelength generation in the mid-IR spectrum. In particular, OPGs can be attractive, owing to their simple, compact and robust architecture. An OPG typically constitutes a pump laser and a nonlinear crystal in a traveling-wave configuration [3]. The nonlinear optical process involves a three-wave interaction initiated by the pump, leading to the macroscopic generation of signal and idler radiation at the output of the nonlinear crystal. As a result of the single-pass interaction, the OPG requires high-intensity laser pump sources and suitable materials with sufficiently high optical damage tolerance. An interesting and practical approach to generate mid-IR wavelengths beyond 5 μm would be to drive OPGs by direct deployment of high-energy, Nd-based solid-state laser pump sources near 1 μm. However, to date, this has proved challenging due to the stringent material requirements. Mid-IR spectral regions up to ~4 μm can be readily accessed by exploiting oxide-based periodically-poled materials such as MgO:PPLN and MgO:PPPLT, which offer moderate nonlinear coefficients ( $d_{\text{eff}} \sim 10\text{--}16$  pm/V) and, importantly, a wide bandgap, enabling pumping using the well-established Nd-based solid-state and Yb-based fiber lasers near 1 μm [6,7]. However, spectral coverage significantly beyond 4 μm is limited by the multiphonon absorption at the generated idler wavelengths in the mid-IR. This sets a practical upper limit of ~4 μm for parametric generation in oxide-based crystals, and so alternative nonlinear materials must be explored. Table 1 lists the pertinent characteristics of a number of important mid-IR nonlinear crystals [8]. The materials, which must primarily be non-centrosymmetric, should have a sufficiently large bandgap to extend the transparency range from near-IR into the deep mid-IR. They should also offer relatively large optical nonlinearity with good thermal and mechanical properties, mandatory for practical realization of parametric sources. Among potential nonlinear material candidates for mid-IR wavelength generation beyond ~4 μm is ZnGeP<sub>2</sub>, which is a well-established chalcopyrite crystal with wide transparency extending across 0.7–12 μm and possesses high optical nonlinearity. However, pumping near 1 μm in this material is precluded by two-photon absorption, necessitating long-wavelength pump sources beyond ~2 μm. Similarly, other chalcopyrite materials such as silver gallium selenide, AgGaSe, and the vast majority of other chalcogenide-based mid-IR nonlinear materials, suffer from two-photon absorption for pumping near 1 μm. While silver thiogallate, AgGaS<sub>2</sub>, can be phase-matched for pumping near 1 μm, it has relatively low nonlinearity and poor thermal conductivity. Orientation-patterned gallium arsenide, OP-GaAs, is another important nonlinear material for parametric generation in the mid-IR, offering wide transparency and high nonlinearity. However, its low bandgap energy similarly poses a limitation for pumping near 1 μm, due to two-photon absorption, thus requiring long-wavelength pump sources near 2 μm. While cascaded pumping schemes using primary laser sources near 1 μm can offer an alternative approach to mid-IR generation beyond 4 μm in such non-oxide materials, the

direct deployment of single-step pumping offers potential advantages of reduced complexity and increased conversion efficiency. It would thus be imperative to continue the search for new nonlinear materials for practical generation of mid-IR radiation beyond 4  $\mu\text{m}$  using direct pumping with the well-established Nd-based solid-state lasers near 1  $\mu\text{m}$ .

**Table 1. Properties of Major Mid-IR Nonlinear Materials [8].**

|   | MgO:PPLN                      | ZnGeP <sub>2</sub>             | AgGaS <sub>2</sub>             | OP-GaAs                       | CdSiP <sub>2</sub>             |
|---|-------------------------------|--------------------------------|--------------------------------|-------------------------------|--------------------------------|
| Transparency ( $\mu\text{m}$ )                | 0.3-5                         | 2-12                           | 0.5-11.4                       | 1.1-17                        | 1-6.5                          |
| Nonlinear coefficient (pm/V)                  | 16<br>(@ 1 $\mu\text{m}$ )    | 70<br>(@ 5.3 $\mu\text{m}$ )   | 13.7<br>(@ 2.5 $\mu\text{m}$ ) | 119<br>(@ 1.5 $\mu\text{m}$ ) | 84.5<br>(@ 4.5 $\mu\text{m}$ ) |
| Bandgap (eV)                                  | 4                             | 2                              | 2.7                            | 1.4                           | 2.2                            |
| Phase-matching for pumping at 1 $\mu\text{m}$ | ✓                             | ✗                              | ✓                              | ✗                             | ✓                              |
| Two-photon absorption coefficient (cm/GW)     | 0.1<br>(@ 0.5 $\mu\text{m}$ ) | 0.25<br>(@ 1.3 $\mu\text{m}$ ) | 0.18<br>(@ 0.8 $\mu\text{m}$ ) | 20<br>(@ 1 $\mu\text{m}$ )    | 2.4<br>(@ 1 $\mu\text{m}$ )    |
| Thermal conductivity (W/m-K)                  | 4.6                           | 36                             | 1.5                            | 52                            | 13.6                           |

The newly developed mid-IR nonlinear crystal, cadmium silicon phosphide, CdSiP<sub>2</sub> (CSP), is a negative uniaxial chalcopyrite semiconductor belonging to the space group  $\bar{4}2m$ , with practical transparency extending from 1 to 6.5  $\mu\text{m}$  [9]. Uniquely and importantly, the linear and nonlinear optical properties of CSP permit parametric generation under noncritical phase-matching (NCPM) with a large effective nonlinearity ( $d_{\text{eff}} \sim 84$  pm/V), providing mid-IR idler radiation near 6  $\mu\text{m}$  when pumped at 1064 nm [10]. Its nonlinear figure of merit,  $F = d_{\text{eff}}^2/n^3$ , with  $n \sim 3.1$ , is nearly ten times greater than MgO:PPLN. Further, CSP has a small, but finite, thermal dependence of the refractive indices, enabling temperature tuning. The possibility of pumping CSP at the well-established Nd:YAG wavelength of 1.064  $\mu\text{m}$  to generate mid-IR radiation at mid-IR wavelengths as far as 6  $\mu\text{m}$  in a simple and robust OPG scheme is one of the most important features of this new nonlinear material.

Earlier reports of parametric devices based on CSP pumped near 1  $\mu\text{m}$  include nanosecond OPOs [11,12] and picosecond OPOs [13,14]. Also, a mid-IR OPG based on CSP pumped by a picosecond amplified mode-locked Nd:YVO<sub>4</sub> laser at 1.064  $\mu\text{m}$  has been reported, providing a fixed output wavelengths, and generating an idler energy up to 1.54  $\mu\text{J}$  at 6.204  $\mu\text{m}$  together with signal energy of 11.6  $\mu\text{J}$  at 1.282  $\mu\text{m}$  [15].

Here we report, for the first time to our knowledge, a picosecond OPG based on CSP pumped at 1.064  $\mu\text{m}$ , capable of providing record pulse energies and broad wavelength tuning in the mid-IR. The OPG is tunable over 6153-6732 nm (idler) in the mid-IR and 1264-1286 nm (signal) in the near-IR, and can deliver  $\sim 600$   $\mu\text{J}$  of output energy over the entire signal tuning range in 24 ps pulses together with  $>25$   $\mu\text{J}$  of long-wavelength mid-IR pulse energy over 55% of the idler tuning range.

## 2. Experimental setup

### 2.1 Pump laser

The schematic of the laser system together with the experimental setup for the OPG is shown in Fig. 1. The pump laser is a laboratory designed oscillator-amplifier system operating at a wavelength of 1.064  $\mu\text{m}$  [16]. The active medium in the laser oscillator is 30-mm-long Nd:YAG slab, with Nd doping concentration of 2.4 at.%. The two end faces with an aperture of  $5 \times 2$  mm<sup>2</sup> were cut at the Brewster angle of 68°. The pumping face has an aperture of  $30 \times 2$  mm<sup>2</sup> and is antireflection (AR) coated at 808 nm. The pump source for the oscillator is a single quasi-continuous-wave laser diode (LD) bar with the fast axis collimation, providing a nominal output power of 150 W at a repetition rate of 100 Hz. The LD is mounted on a copper plate with Peltier cooling, enabling fine tuning of output wavelength around 808 nm to

match the Nd:YAG absorption peak. The oscillator is configured in a standing-wave cavity formed by the mirrors,  $M_1$ - $M_3$ , and a semiconductor saturable absorber mirror (SAM).  $M_1$  is an AR coated plane mirror with reflectivity of  $\sim 70\%$  at 1064 nm.  $M_2$  is a plano-concave mirror with radius of curvature of 1 m, while  $M_3$  is a plane mirror, both high reflecting at 1.064  $\mu\text{m}$ . The total physical length of the optical resonator is 1.12 m, corresponding to free spectral range of 131 MHz. The laser is optimized for operation in the passive mode-locking regime at a wavelength of 1.064  $\mu\text{m}$ , using a SAM with a modulation depth of 25%. In order to extract a single pulse from the Q-switched mode-locked output train, the oscillator is cavity dumped using a KD\*P Pockels cell and a Glan laser polarizer. The residual transmission from  $M_1$  is used to trigger a high voltage quarter-wave step signal (rise time below 7 ns) for the Pockels cell. The oscillator generates vertically polarized single pulses with energy of  $25 \pm 2 \mu\text{J}$ . The output beam spatial profile is nearly Gaussian in both axes, and the duration of the output pulses measured by the streak camera is 20 ps with stability better than 2 ps. The pump pulse energy is further boosted up to 2.5 mJ by a single-pass flashlamp-pumped amplifier based on 100-mm-long Nd:YAG crystal with no significant effect on pulse duration. The pulse repetition rate after the amplifier is limited to 5 Hz by the flashlamp power supply.

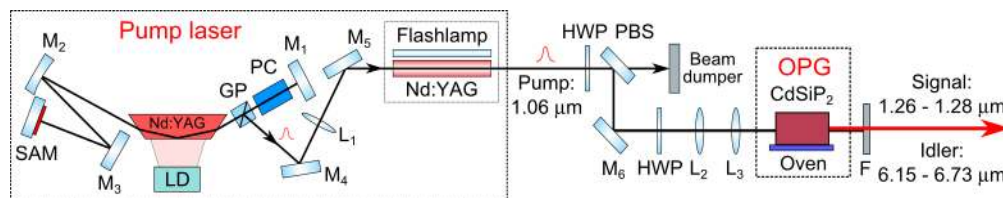


Fig. 1. Schematic of the experimental setup for CSP OPG. SAM: Saturable absorber mirror, LD: Laser diode, PC: Pockels cell, GP: Glan polarizer, HWP: Half-wave-plate, PBS: Polarizing beam splitter, M: Mirrors, L: Lens, F: Filter.

## 2.2 Optical parametric generator

The output beam from the laser at a wavelength of 1.064  $\mu\text{m}$ , with a diameter of 2 mm and a beam quality factor of  $M^2 \sim 1.8$ , is used to pump the OPG. The nonlinear crystal is a 12.1-mm-long, 4-mm-wide (along the  $c$ -axis), 5-mm-thick CSP sample grown from stoichiometric melt by the horizontal gradient freeze technique [9]. It is cut at  $\theta = 90^\circ$ ,  $\phi = 45^\circ$  for type-I ( $e \rightarrow oo$ ) interaction under NCPM and housed in an oven whose temperature can be varied from room temperature to 200  $^\circ\text{C}$  in steps of  $\pm 0.1 \text{ }^\circ\text{C}$ . Both crystal faces are AR coated with a single-layer sapphire, providing high transmission,  $T > 98.7\%$  for the pump and signal over 1064-1300 nm and  $T > 76\%$  for the idler over 6000-6500 nm. The pump beam is collimated to a beam radius of 700  $\mu\text{m}$  at the center of the nonlinear crystal. The beam waist is optimized to use the maximum available pump pulse energy and yet to avoid potential damage to the CSP crystal or the coating. The generated signal is separated from the residual pump using a near-IR filter, while a germanium filter is used to extract the mid-IR idler output.

## 3. Results and discussion

### 3.1 Temperature tuning

In order to characterize the OPG with regard to wavelength tunability, we initially performed temperature tuning measurements. The temperature of the nonlinear crystal was varied by altering the set-point temperature of the oven. We used an additional thermocouple, connected directly to the crystal holder, to accurately monitor the actual crystal temperature. The variation of the oven temperature from 25 to 200  $^\circ\text{C}$  corresponded to a thermocouple temperature variation from 25 to 174  $^\circ\text{C}$ , indicating that the set-point temperature of the oven differs significantly from the real crystal temperature at high temperatures. Hence, by changing the temperature of the CSP crystal from 25 to 174  $^\circ\text{C}$ , we were able to tune the OPG over 1263-1286 nm (23 nm) in the near-IR signal, corresponding to 6731-6153 nm (578 nm)

in the mid-IR idler. Figure 2(a) shows the temperature tuning curves of the CSP OPG. The signal wavelength was recorded by using an InGaAs spectrometer (Ocean Optics, NIR 512,

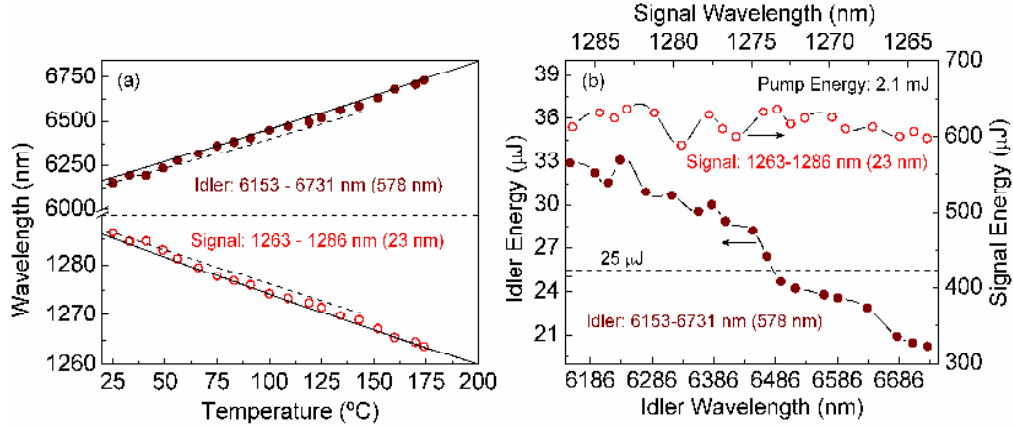


Fig. 2. (a) Temperature tuning curves, (b) extracted signal and idler energy across the tuning range of the CSP OPG.

resolution  $\sim 5$  nm), and was further confirmed by single-pass second harmonic generation into the red in a 10 mm  $\text{LiIO}_3$  crystal with type-I ( $oo \rightarrow e$ ) phase-matching. The corresponding idler wavelength was inferred from energy conservation. The solid line in Fig. 2(a) is the theoretical tuning curve calculated from the Sellmeier equations for CSP [9], while the dashed line is calculated from the Sellmeier equations reported recently [17]. As evident from Fig. 2(a), the theoretical solid lines are in close agreement with our experimentally measured data. The amount of signal and idler energy extracted over the entire tuning range is shown in Fig. 2(b). For a fixed pump energy of 2.1 mJ at the input to the CSP crystal, the signal energy remains almost constant at  $\sim 600$   $\mu\text{J}$  over the entire tuning range, while the idler energy varies from a maximum of 33  $\mu\text{J}$  at 6153 nm to 20  $\mu\text{J}$  at 6731 nm, providing  $>25$   $\mu\text{J}$  over 55% of the tuning range. The drop in the idler energy towards the longer wavelengths is attributed to water absorption peak near 6.4  $\mu\text{m}$  and residual multi-phonon absorption in the CSP crystal, resulting in reduced transmission.

### 3.2 Energy scaling

We also characterized the OPG for energy scaling at a temperature of 91°C, corresponding to an idler wavelength near 6400 nm. Under this condition, we were able to generate as much as 600  $\mu\text{J}$  of signal at 1276 nm, together with 30  $\mu\text{J}$  of idler at 6404 nm, for input pump energy of 2.1 mJ, as shown in Fig. 3. This represents an energy conversion efficiency of 28.6% and a photon conversion efficiency of 34.2% for the signal. Similarly, the idler is recorded to have an energy conversion efficiency of 1.4% and photon conversion efficiency as high as 8.6% at wavelengths as long as 6404 nm. The corresponding slope efficiencies extracted from the linear fits to the experimental data for the signal and idler are 30% and 14%, respectively. The threshold pump energy of the OPG is recorded to be  $\sim 120$   $\mu\text{J}$ , corresponding to a peak intensity of  $\sim 0.4$   $\text{GW}/\text{cm}^2$ . The threshold pump intensity for superfluorescence generation starting from quantum noise is given by Eq. (1) [18,19]

$$I_{th} \approx 5 \frac{\epsilon_0 c n^3 \lambda_s \lambda_i}{d_{eff}^2 L^2} \quad (1)$$

where  $\epsilon_0$  is the permittivity of free space,  $c$  is the velocity of light,  $n$  is the refractive index of the material,  $\lambda_s$  is the signal wavelength (1276 nm),  $\lambda_i$  is the idler wavelength (6404 nm). For a

12-mm-long CSP crystal, with  $d_{\text{eff}} \sim 84$  pm/V, a signal wavelength of 1276 nm and an idler wavelength of 6404 nm, the threshold intensity predicted by Eq. (1) is  $\sim 0.3$  GW/cm<sup>2</sup>, which

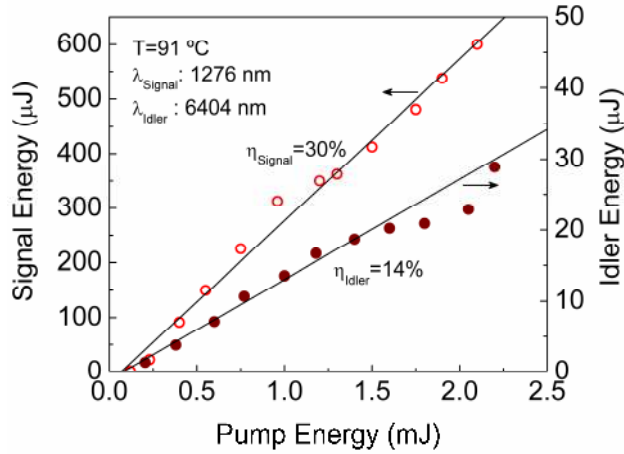


Fig. 3. Variation of the signal (1276 nm) and idler (6404 nm) energy extracted from CSP OPG as a function of the pump energy.

is slightly lower than the experimentally measured pump threshold of  $\sim 0.4$  GW/cm<sup>2</sup>. The difference in the theoretically predicted and experimentally measured threshold intensity can be attributed to the residual losses at pump, signal and idler wavelengths in the CSP crystal. Although the losses due to multi-phonon absorption, which limit the long-wavelength transparency in CSP, are intrinsic, the residual absorption close to the bandgap of the material, limiting the short-wavelength transparency, is not intrinsic. Hence, progress in the crystal growth technology, leading to improvement in the optical quality of the CSP crystal, could further reduce the parametric generation threshold.

### 3.3 Temporal and spectral characterization

Further, we performed spectral and temporal characterization of the signal pulses generated from the OPG. Figure 4(a) shows a typical autocorrelation profile measured at a temperature of 91 °C, corresponding to a signal wavelength of 1276 nm. The FWHM of the curve is 34 ps, resulting in signal pulse duration of 24 ps, assuming a Gaussian pulse shape. This value of the pulse duration was confirmed by repeating the measurement several times. The corresponding signal spectrum measured using a near-IR spectrometer is centered at 1276 nm with a FWHM bandwidth of 10.4 nm, as shown in Fig. 4(b), resulting in  $\Delta\nu\Delta\tau \sim 46$ . The large time-bandwidth product is attributed mainly to power broadening due to the OPG operation  $\sim 18$  times above threshold, as well as non-collinear generation. Additionally, we have recorded the idler spectrum at the same temperature of 91 °C using a grating spectrometer. The measured idler spectrum centered at 6404 nm is shown in Fig. 5 and has an FWHM bandwidth of 140 nm.

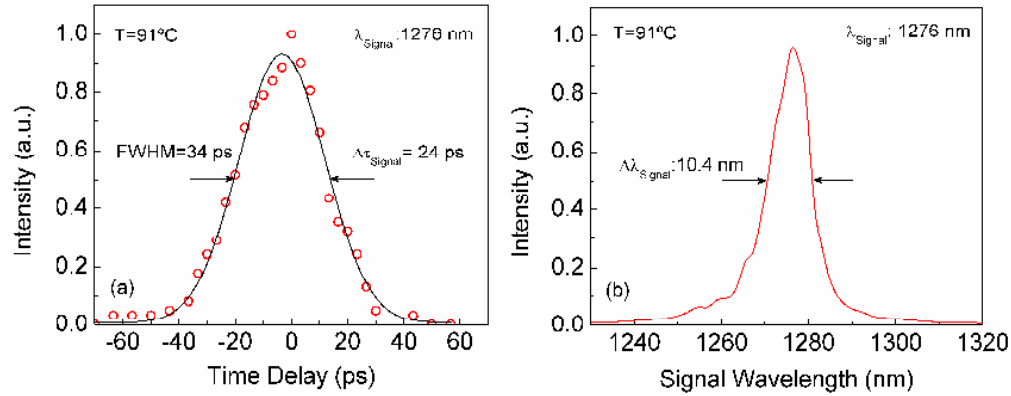


Fig. 4. (a) Typical autocorrelation and (b) spectrum of the CSP OPG signal pulses at 1276 nm.

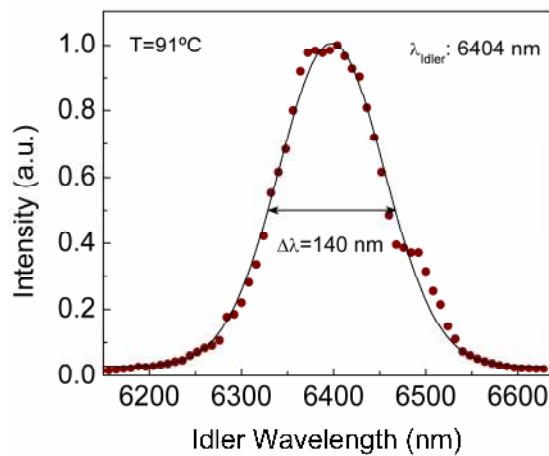


Fig. 5. Spectrum of the idler pulses generated from the CSP OPG centered at 6404 nm.

#### 4. Conclusions

In conclusion, we have demonstrated a tunable, high-energy, picosecond single-pass OPG with record near-IR signal and mid-IR idler pulse energy based on the new nonlinear material, CSP. This is the first demonstration of tunable OPG based on CSP, to the best of our knowledge. The OPG signal is tunable over 1263-1286 nm in the near-IR, generating 24 ps pulses with output energies as much as 600  $\mu$ J over the entire tuning range. The corresponding idler is tunable over 6153-6731 nm in the mid-IR, providing maximum pulse energy of 33  $\mu$ J at 6153 nm. The spectral measurements of the idler resulted in a broadband spectrum with a FWHM bandwidth of 140 nm centered at 6404 nm.

#### Acknowledgments

We acknowledge support for this research by the European Union 7th Framework Program MIRSURG (grant 224042), partial support by the Ministry of Science and Innovation, Spain, through Consolider Program SAUUL (grant CSD2007-00013), the Catalan Agència de Gestió d'Ajuts Universitaris i de Recerca (AGAUR) through grant SGR 2009-2013 and plan nacional through grant FIS2011-30465-C02-01. Funding from LASERLAB-EUROPE (228334) as well as Czech Science Foundation under grants No. 102/12/2361 and 102/09/1741 is also gratefully acknowledged.